J. Appl. Comput. Mech., 6(3) (2020) 582-592
DOI: 10.22055/JACM.2019.29201.1571

ISSN: 2383-4536
jacm.scu.ac.ir

M&MoCS

Shahid Chamran University of Ahvaz

Journal of Applied and Computational Mechanics

Research Paper

Prediction of Entrance Length for Magnetohydrodynamics Channels Flow using Numerical simulation and Artificial Neural Network

Mohammad Hasan Taheri, Nematollah Askari, Mohammad Hadi Mahdavi

Department of Mechanical Engineering, Faculty of Imam Khomeini, Behshahr Branch, Technical and Vocational University (TVU), Mazandaran, Iran

Received April 17 2019; Revised May 10 2019; Accepted for publication May 15 2019.
Corresponding author: Mohammad Hasan Taheri (hasan.taheri@gmail.com)

Abstract. This paper focuses on using the numerical finite volume method (FVM) and artificial neural network (ANN) in order to propose a correlation for computing the entrance length of laminar magnetohydrodynamics (MHD) channels flow. In the first step, for different values of the Reynolds (Re) and Hartmann (Ha) numbers (600<Re<1100 and 4<Ha<10), FVM was carried out and the values of entrance length were obtained. The hybrid and central differencing schemes were used for the convective and diffusive terms, respectively. Also, the SIMPLE algorithm was selected for solving the pressure field. In the second step, a feed-forward back-propagation ANN was trained. Then, the trained ANN was applied to develop the datasets for a wide range of Re and Ha. In the last step, using a fitting tool, the correlations for computing the MHD entrance length of channels were obtained. It was shown that by increasing of Ha, the MHD entrance length declined. However, when Re increases, the MHD entrance length is increased. In additions, with the increase of Ha, the velocity profile gets flatten and consequently, the entrance length becomes shorter. Further, the effect of Ha on the Lorentz force was discussed. It was shown that with increasing of Ha, F_L increases.

Keywords: Artificial neural network, Channel, Magnetohydrodynamics, MHD entrance length, Numerical simulation.

1. Introduction

Magnetohydrodynamics (MHD) has been a subject of great researches due to its importance in the plentiful fields such as natural phenomena like geophysics and astrophysics, many engineering applications like plasma confinement, electromagnetic stirring and magnetic damping in casting operations, electrolysis and so on [1-11]. The fluid flow in the presence of a transverse magnetic field occurs in metallurgical industries processing applications, electromagnetic pump and within the liquid metal cooling of reactors. Well-estimate of the MHD channel's entrance length is not only useful for fluid engineers to design relevant systems, but also necessary for scientist to solve critical issues in this field. The control of electrically conducting fluids is getting more important in recent years. Using the MHD flow is one of the common methods. The magnetic field develops the resistance Lorentz force that is dissipative in nature, so it can be used to suppress the velocity fluctuations.

The literature survey reveals that the most of the researches in the field of the MHD developing channel flow have been done either numerically or experimentally for different Hartmann numbers and uniform or parabolic entrance velocity profile. However, a few analytical investigations were carried out in the field of MHD entrance channel flow. Using of the integral methods to solve the laminar boundary layer equations are widely applied in MHD channels studies [12-17]. In these researches, the two dimensional laminar flow of an incompressible conducting fluid between two parallel flat plate was considered. The applied magnetic field was assumed uniform in the direction normal to the

Published online: September 21 2019

flow. The induced magnetic field was neglected, due to the small magnetic Reynolds number. For each case, the velocity distribution and the boundary layer thickness were obtained. Lima and Rego [18] presented the hybrid numerical-analytical approach known as GITT (Generalized Integral Transform Technique) and solved the flow and heat transfer for an MHD channel, sustained by a pressure gradient subjected to a uniform magnetic field.

The numerical studies of the MHD developing flows can be carried out using several techniques such as the finite difference method, finite volume method and finite element method etc. Hwang et al. [19] employed a finite difference analysis to study the laminar MHD entrance flow in a flat channel with parabolic inlet velocity. They showed that the considered inlet velocity, which is the velocity profile for a fully developed non-magneto hydrodynamic laminar flow, eventually develops into the Hartmann velocity profile in the entrance region of a channel in presence of a uniform magnetic field. The entrance length, pressure drops and developing velocity profiles were computed numerically for the Hartmann number of 2.5,4,10 and 50. Flores and Recuero [20] investigated an MHD entrance flow in a plane channel with the Prandtl approximation. They established a modified boundary condition for the problem and concluded that as the Hartmann number increases, the entrance length decreases. Besides, they reported the modified boundary condition affects more strongly the solution. Bhuyan and Goswami [21] investigated a one-dimensional incompressible laminar flow of a liquid metal in a rectangular duct under the influence of a transverse magnetic field, numerically. The governing equations were solved using control-volume techniques over non-uniform plane grids. Simulations have been performed for channels with and without electrical insulation, and the pressure drop is evaluated for each case. In additions, the effect of Hartmann number and walls conductivity on the flow field were discussed. Sahu et al. [22] proposed an adaptive network fuzzy inference system (ANFIS) to predict the entrance length in pipes for low Reynolds number developing flow under various working condition. The CFD techniques have been adopted to generate required data. The flow is considered steady and incompressible without swirl and the examined fluids were water and air.

Li and Zikanov [23] analyzed the three-dimensional transition flow of a liquid metal in a pipe at the entrance under a transverse magnetic field. They considered the case of the laminar flow, the perfectly insulating pipe walls and the Hartmann number up to 200. The simulations revealed detailed structure of the velocity and the electric current fields and the distribution of the forces. They also established criteria of the accurate computations of the laminar MHD flows in the strong non-uniform magnetic fields. Patel et al. [24] carried out an experimental investigation of liquid metal MHD flows with non-magnetic and ferro-magnetic test sections. The wall electrical potential and MHD pressure drop across the test sections were compared under identical experimental conditions. It was concluded that the similar MHD behavior is observed with both the test sections at higher value of the magnetic field. Kim [25] examined the three-dimensional developing liquid metal MHD flows entering the region of the flow channel insert (FCI) under a uniform magnetic field, numerically. The velocity was assumed parabolic at the entry. The features of the flows in a square channel near the leading edge of the FCI were studied in terms of the flow velocity, the pressure, the current, the electric potential and the Lorentz force. Satyamurthy et al. [26] performed an experimental study of the MHD flows on a stainless steel test section with parallel channels and sub-ducts. In addition, they presented a numerical solution for the corresponding experimental flow rates and applied magnetic field using a finite volume based CFD solver Ansys Fluent. The main results included the pressure drop, the flow rate, the velocity and the side-wall electric potential distributions. They reported that the Fluent numerical results are in good agreement with the experimental data and the deviation was less than or close to the experimental errors.

Chatterjee and Gupta [27] simulated the two-dimensional MHD flow of liquid metal around a square object placed in a square duct under a strong homogeneous magnetic field numerically using Ansys Fluent (version 14). A wide range of the Reynolds and the Hartmann numbers were considered. Jasikova et al. [28] examined an effect of the entrance length on the development of the velocity profile in a polycarbonate plastics plane channel of millimeter dimensions. The experimental results including the flow stability and velocity profile shape in the channel of 0.00375 hydraulic diameters. A range of the entrance length for the transient flow area was marked and the minimal entrance length for the laminar, transition, and turbulent flow was set. Kountouriotis et al. [29] studied the flow development of a Newtonian fluid in both channels and tubes with Navier's slip flow assumption, numerically. Two definitions of the entrance length. Results were obtained for a wide range of the Reynolds and the slip numbers. They concluded that the flow development in the channel is slower near the wall than at the mid plane in the presence of the finite slip.

In recent decade, the Artificial Neural Network (ANN) has gained considerable attention as a predictive tool because of their special benefits. Jambunathan et al. [30] applied Neural Networks based on the back-propagation algorithm to predict heat transfer coefficients from given sets of the experimental data. The study on the performance characteristics for numerous network configurations yielded the optimal network layers, neurons arrangement and the least error. Sözbir et al. [31] studied an artificial neural network for the prediction of unsteady heat transfer in a plane channel. An experimental study was carried out to investigate the axial variation of inlet temperature and the impact of inlet frequency on decay indices in the thermal entrance region of a parallel plate channel. The investigation was conducted with laminar forced flows for specified range of the Reynolds number and the inlet heat frequency. The results revealed that the ANNs can be used for modeling unsteady heat transfer in channels. Diaz et al. [32] used the artificial neural network technique for prediction of the heat transfer coefficient through a fin-tube heat exchanger. Two cases of convective heat transfer with one and two heat transfer coefficients were examined, and more required data was generated artificially. Finally, the method was applied to analysis the data obtained in the laboratory for a single-row fin-tube heat exchanger. It was shown that a better prediction with smaller scatter is obtained in comparison to a conventional power-law correlation for the heat transfer coefficients. Carrillo et al. [33] employed artificial neural networks in order to obtain the estimation of Reynolds number in a two-dimensional Poiseuille flow. The flow velocity was generated with evaluating the Hage-Poiseuille equation for different Reynolds from 20 to 2000. The velocity profile obtained for each case is used as input data for the ANNs, which is then trained to predict the Reynolds number. The results show an acceptable accuracy in all prediction cases.

However, although the MHD developing flows was investigated for several cases and different applications in the past decades, but little attention has been paid to introduce the precise correlation for the entrance length of MHD channels flow. Besides, the artificial neural network (ANN) has not been utilized yet in this field. In this paper, a new solution based on the numerical simulation and artificial neural network (ANN), with the aim of obtaining the correlations for computing the MHD entrance length is presented. The two-dimensional, steady state, laminar flow of an electrically conducting fluid through an MHD plane channel is investigated, and the effect of the different parameters on the MHD entrance length are discussed.

2. Problem Statement

In Fig. 1, the problem under consideration is presented schematically. The steady flow of a viscous, incompressible and electrically conducting fluid (liquid metal), in a two- dimensional channel is considered. The length of the channel is L=0.7m (x-direction), while the width is W=0.01m (y-direction). The depth of the channel (z-direction) is long enough in comparison of the width, so it will not affect the velocity profile. There is no-slip condition on the walls.
A liquid metal flow with uniform velocity enters the channel. After passing the specified length of the channel, the flow becomes fully developed and the inlet velocity distribution changes to parabolic form, which is the hydrodynamically fully developed velocity profile. As shown in Fig. 1, a uniform magnetic field perpendicular to the channel, imposes on the flow after a distance x_0 far from the entry. So, the parabolic velocity profile eventually develops into the MHD fully developed velocity profile (u_{cm}) in the presence of magnetic field. The distance along the channel length, where the centerline velocity reaches 99% of its final MHD fully developed value is defined as the MHD entrance length.
The governing equations for described problem are continuity, momentum and Ohm's law introduced as [12]:

$$\nabla.\vec{V} = 0 \tag{1a}$$

$$\rho\left(\vec{V}.\nabla\right)\vec{V} = -\nabla\vec{P} + \mu\nabla^2\vec{V} + \sigma\left(\vec{J}\times\vec{B}\right) \tag{1b}$$

$$\vec{J} = \sigma\left(\vec{E} + \vec{V}\times\vec{B}\right) \tag{1c}$$

where V, E, J, B and P are the velocity field, electric field, electric current density, total magnetic field and gauge pressure, respectively. All fluid properties are assumed constant and the effect of gravity is neglected. The volumetric Lorentz force is given as [12, 34]:

$$\vec{F}_L = \vec{J}\times\vec{B} = \sigma\left(\vec{E} + \vec{V}\times\vec{B}\right)\times\vec{B} \tag{2}$$

which total magnetic field (B=B_0+b) is sum of the applied (B_0) and induced (b) magnetic field. The electric field term is zero and the magnetic Reynolds number is assumed small, indeed the induced magnetic field is neglected in comparison with the applied magnetic field. Therefore, the volumetric Lorentz force is [12, 35]:

$$\vec{J}\times\vec{B} = -\sigma B_0^2 u\vec{i} \tag{3}$$

Under the above assumptions, Eqs. (1) are simplified as follow:

$$\frac{\partial u}{\partial x} + \frac{\partial v}{\partial y} = 0 \tag{4a}$$

$$\rho\left(u\frac{\partial u}{\partial x} + v\frac{\partial u}{\partial y}\right) = -\frac{\partial P}{\partial x} + \mu\left(\frac{\partial^2 u}{\partial x^2} + \frac{\partial^2 u}{\partial y^2}\right) - \sigma B_0^2 u \tag{4b}$$

$$\rho\left(u\frac{\partial v}{\partial x} + v\frac{\partial v}{\partial y}\right) = -\frac{\partial P}{\partial y} + \mu\left(\frac{\partial^2 v}{\partial x^2} + \frac{\partial^2 v}{\partial y^2}\right) \tag{4c}$$

where u is the velocity in x direction and v is the velocity in y direction. The boundary conditions for described problem are defined as:

$$x = 0 \;\rightarrow\; u = u_c\left[1 - \left(\frac{y}{0.005}\right)^2\right],\; v = 0 \tag{5a}$$

$$y = \pm 0.005 \quad \rightarrow \quad u = v = 0, \tag{5b}$$

$$x = 0.7 \quad \rightarrow \quad P = 0, \frac{\partial u}{\partial x} = 0 \tag{5c}$$

where u_c and Ha are the core centerline velocity and the Hartmann number, respectively. By choosing different values of centerline velocity, different parabolic velocity profile is obtained which conduce specified Reynolds number.

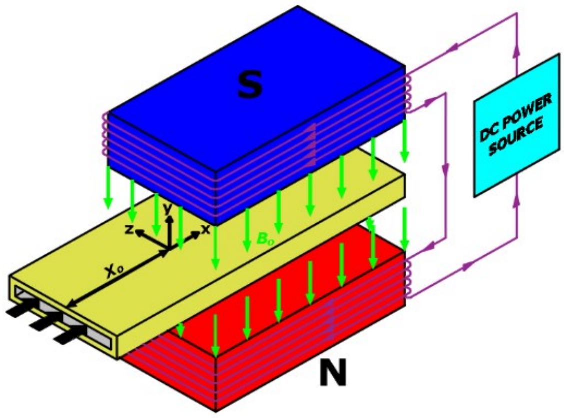

Fig. 1. Problem schematic

By introducing dimensionless parameters as:

$$x' = \frac{x}{D\mathrm{Re}_D}, y' = \frac{y}{D}, \; u' = \frac{u}{U}, v' = \frac{\rho D}{\mu} v, P' = \frac{P}{\rho U^2} \tag{6}$$

The governing equations are transformed into dimensionless form as:

$$\frac{\partial u'}{\partial x'} + \frac{\partial v'}{\partial y'} = 0 \tag{7a}$$

$$u' \frac{\partial u'}{\partial x'} + v' \frac{\partial u'}{\partial y'} = -\frac{\partial P'}{\partial x'} + \left(\frac{1}{(\mathrm{Re}_\ell)^2} \frac{\partial^2 u'}{\partial x'^2} + \frac{\partial^2 u'}{\partial y'^2} \right) - Ha^2 u' \tag{7b}$$

$$u' \frac{\partial v'}{\partial x'} + v' \frac{\partial v'}{\partial y'} = -\frac{\partial P'}{\partial y'} + \left(\frac{1}{(\mathrm{Re}_\ell)^2} \frac{\partial^2 v'}{\partial x'^2} + \frac{\partial^2 v'}{\partial y'^2} \right) \tag{7c}$$

Two dimensionless parameters, which influence the MHD entrance length, included the Reynolds and the Hartmann numbers are defined as follow [34, 36]:

$$\mathrm{Re}_\ell = \frac{\rho u_{av} \ell}{\mu} \tag{8a}$$

$$Ha = B\ell \sqrt{\frac{\sigma}{\mu}} \tag{8b}$$

in which ℓ, the characteristic length for the present work is ℓ=2w. The Reynolds number is the ratio of inertia forces to viscous forces and the Hartmann number is the ratio of the Lorentz force to viscous forces.

3. Methodology

3.1 Finite Volume Method (FVM)

This paper presents a solution based on the numerical simulation and artificial neural network (ANN) in order to obtain a correlation of the MHD entrance length for the two-dimensional MHD channels. In the first place, the numerical simulation is performed to study the liquid metal developing flow through the MHD channel for different values of the Reynolds and Hartmann numbers using finite volume method (FVM). In this step, the investigation is conducted with laminar flows for the Reynolds number ranging from 600 to 1100 while the Hartmann number varied from 4 to 10, and 70 datasets of the MHD entrance length (L_{em}) were generated. Liquid lithium (Li) is selected due to its important application in various industries [37-39]. The hybrid and central difference schemes are used for the convective and diffusive terms, respectively. Also, the SIMPLE algorithm is selected for pressure-velocity coupling and the momentum and continuity equations and the momentum and continuity equations are solved using the Jacobi iterative method. Moreover, to obtain converged results the residual error is selected 10^{-6}. For all calculation, the uniform and rectangular mesh grid are considered in both directions x and y-direction. In order to achieve the valid results, the independence of the results from the mesh is checked. In Table 1, the mesh independent result is shown. It is observed there is no variation in the results for 160×50 grid.

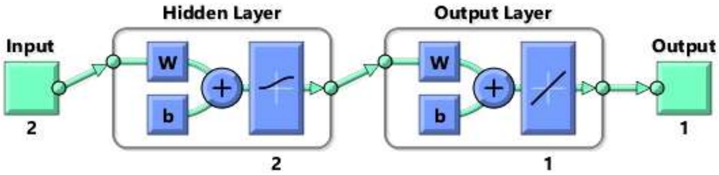

Fig. 2. Structure of the proposed ANN

3.2 Artificial Neural Network (ANN)

Although with the amount of datasets generated from FVM the curve fitting process can be done and a correlation to estimate the MHD entrance length can be obtained, but the suggested correlation will not be accurate. Therefore, in order to obtain a precise correlation for the MHD entrance length, it is necessary to develop the amount of datasets. For this purpose, in the second step, the obtained datasets from the first step are used for the training of ANN.

Table 1. Mesh independence for parabolic inlet velocity

Ha	Re	Mesh number	u_{cm} (m/s)
10	1400	40×25	0.1892
		80×50	0.1901
		160×50	0.1905
		320×100	0.1905

ANNs are nonparametric models that can handle large amount of datasets and they are capable of doing linear and nonlinear regression. ANN model can be adjusted without any need of detailed knowledge of the underlying problem. These unique features have made ANNs applicable in many fields of science.

70 datasets obtained in the first step are used to train in a feed-forward back-propagation network. In this network, the Reynolds and Hartmann numbers are considered as input data and the entrance length is considered as a target data. The schematic of the artificial neural network (ANN) is demonstrated in Fig. 2. Levenberg-Marquardt (LM) algorithm is used to determine the appropriate multi-layer functions for describing the relationship between input and target data.

The sigmoid (log-sigmoid) activation function are applied for the hidden layers and the linear activation function is applied for the output layer, which are expressed mathematically as:

$$\text{Log-sigmoid:} \qquad y_{out} = \frac{1}{1+e^{-x_{in}}} \tag{9}$$

$$\text{Linear:} \qquad y_{out} = x_{in} \tag{10}$$

where x_{in} is the input and y_{out} is the output. For modeling the ANN mathematically, the general expression is defined:

$$y_{out} = f\left(\sum_{j=1}^{n} w_j (x_{in})_j + b\right) \tag{11}$$

where w is the weight, b is the bias and f is the activation function.

The appropriate network can be reached when the mean square error (mse) between the output data and the target is minimized. As the error becomes constant, the training process is stopped (Fig. 3) and the trained network with determined accuracy will be reached. In Table 2 the characteristic of the trained network, the neuron and layer numbers are reported. After that, the trained ANN is applied for the prediction of L_{em} in the previous range of the Reynolds number and Hartmann number ranging from 14 to 20, also for the Reynolds number ranging from 1160 to 2000 while the Hartmann number changed from 4 to 20. After the generation of the required data from ANNs, in the last step, using 300 available datasets, the surface fitting is carried out to obtain a precise correlation for the MHD entrance length of MHD channels.

4. The Proposed Correlation

Applying all steps mentioned in section 3, the MHD entrance length of channel flows as the function of Ha and Re can be obtained as follows:

$$\frac{L_{em}}{D\,\mathrm{Re}_D} = \frac{0.085}{1+0.13Ha^2} \tag{12}$$

$$\frac{L_{em}}{D} = 0.1445 - 0.02273Ha + 0.0006823\,\mathrm{Re} + 0.0006303Ha^2 - (1.624\times10^{-5})\,\mathrm{Re}\,Ha - (1.855\times10^{-7})\,\mathrm{Re}^2 + (2.1\times10^{-5})Ha^3 - (1.038\times10^{-6})Ha^2\,\mathrm{Re} + (1.541\times10^{-8})Ha\,\mathrm{Re}^2 \tag{13}$$

To validate the proposed correlations, Table 3 is presented. It can be observed, the proposed correlations have an acceptable accuracy. In additions, the comparison between the results obtained from the Eqs. 12 and 13 with the FVM and ANN results are presented in Table 4. It can be observed that there is a good agreement between the results. So, the ANN can be a reliable tool for developing the data in a simple way by spending a short time.

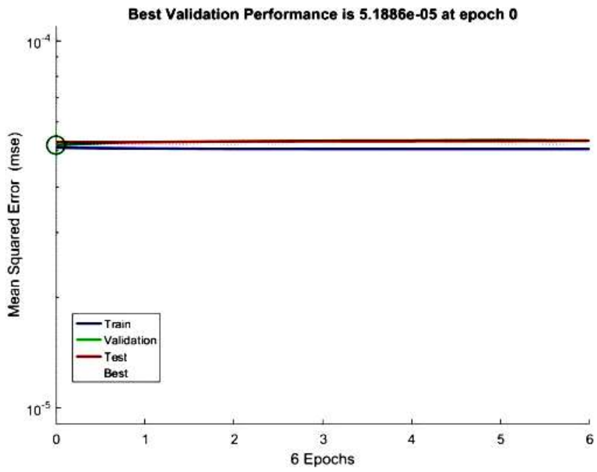

Fig. 3. Neural Network training performance

Table 2. Characteristic of the trained network

Layers number	Training function	Neurons number	Ha range	Re range
2	1st layer: Log-sigmoid 2nd layer: pure line	1st layer: 2 2nd layer: 1	4-10	600 – 1100

Table 3. Validation of the proposed correlation

Re	Ha	L_{em}/D.Re			
		Eq. (12)	Eq. (13)	Hwang et al. [19]	Flores et al. [20]
800	4	0.056	0.059	0.057	0.06
1200	4	0.056	0.059	0.057	0.064
900	10	0.037	0.039	0.036	0.04
1800	10	0.037	0.039	0.036	0.04

Table 4. Comparison of the obtained results from proposed correlations with numerical and ANNs results

Re	700				1400			
Ha	FVM	ANN	Eq. (12)	Eq. (13)	FVM	ANN	Eq. (12)	Eq. (13)
7	0.348	0.349	0.347	0.312	0.596	0.598	0.597	0.625
8	0.323	0.325	0.323	0.292	0.572	0.575	0.572	0.585
9	0.300	0.301	0.299	0.275	0.547	0.550	0.548	0.550
10	0.277	0.279	0.277	0.259	0.522	0.525	0.523	0.519
11	0.255	0.258	0.256	0.246	0.497	0.498	0.496	0.491
12	0.235	0.238	0.236	0.231	0.471	0.472	0.470	0.467

5. Results and Discussions

Figs. 4 (a and b) present the development of the MHD centerline velocity (u_{cm}) in the direction of flow along the channel for different Reynolds and Hartmann numbers. It can be seen that by increasing of the Reynolds number the flow reach to fully developed condition later (Fig. 4a). It happens because as Reynolds number increases, the boundary layers thickness decreases which leads to the increasing of the MHD entrance length. Whereas, with increasing of the Hartmann number, the flow reaches to fully developed condition sooner (Fig. 4b). The Hartmann number represents the ratio of the Lorentz force (F_L) to the viscous force (F_μ). The Lorentz force (F_L) is a resistance body force and proportional to the velocity value. Indeed, when F_L rise up far from the wall the MHD entrance length decreases due to the increasing in the boundary layer growth.

Figure 5 shows the velocity changes in the flow direction along the channel. The development of the velocity distribution can be observed. In the inlet, the velocity has the parabolic distribution and by moving across the channel the velocity distribution changed until it reaches to the fully developed conditions.

The effect of Hartmann number on velocity profile is plotted in Fig. 6. It can be seen that by increasing of the Hartmann number, the velocity profile becomes flattened. According to Eq. (8), Ha is directly proportional to Lorentz force. Indeed, the augmentation of the Hartmann number leads to grow the Lorentz force, which is the resistance force and apply in the opposite direction of the flow.

In Fig. 7, the variation of the Lorentz force (F_L) in the entrance region of channel is depicted. It can be seen that by moving in the direction of flow along the channel, F_L in centerline of the channel decreases and when the flow becomes fully developed, F_L turns constant. According to Eq. (3), the Lorentz force is proportional to the electrical conductivity (σ), external magnetic field (B_0), and velocity (u). Since σ and B_0 are constant, F_L only depends on u. Therefore, F_L is reduced because of the centerline velocity decreases along the channel.

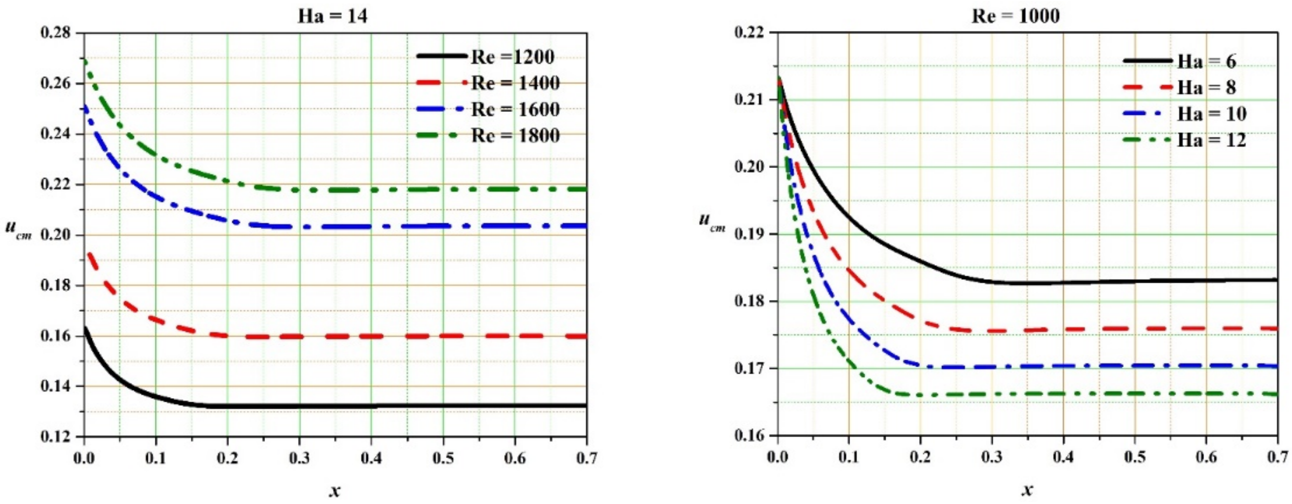

(a) (b)

Fig. 4. Velocity variations along the channel for different values of Ha and Re

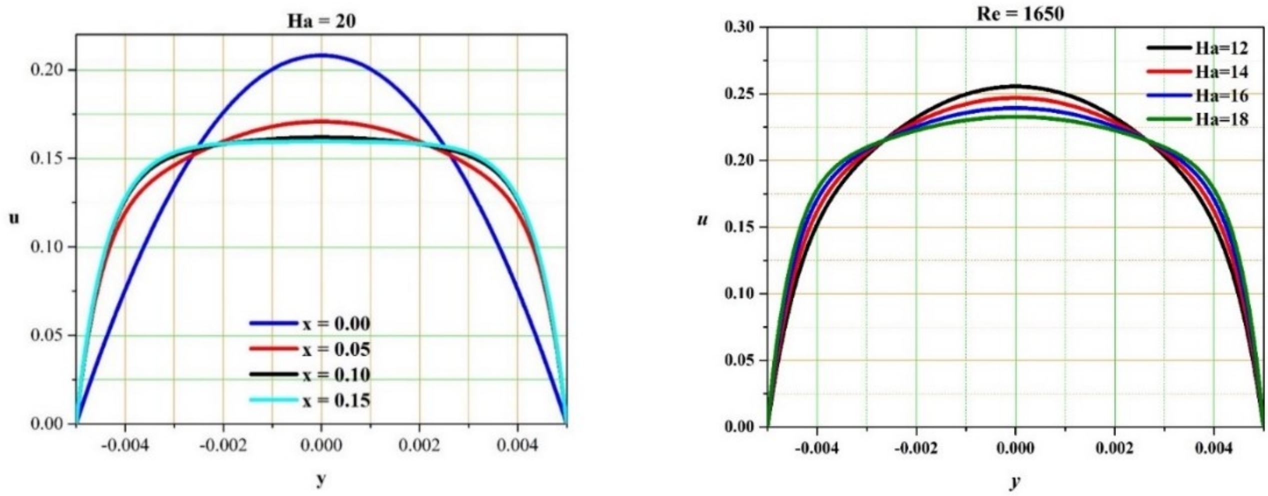

Fig. 5. Velocity distribution along the channel axis (Re = 1167)

Fig. 6. Effect of the Hartmann number on velocity profile

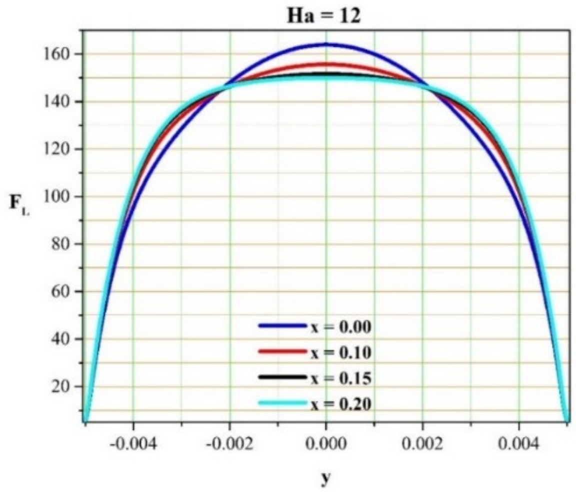

Fig. 7. Distribution of the Lorentz force in the entrance region (Re = 1167)

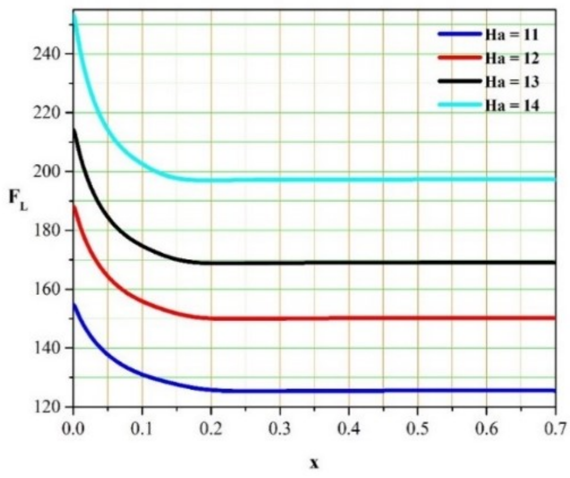

Fig. 8. Effect of the Hartmann number on the Lorentz force (Re = 1167)

The effect of the Hartmann number on Lorentz forces in the centerline of the channel (F_L) is presented in Fig. 8. As mentioned before, the Hartmann number is the ratio of the Lorentz force to the viscous force, so the Hartmann number is directly proportional to the Lorentz force. Thus, as expected, with increasing of the Hartmann number F_L increases.

In order to gain insight into some of the results, the vectors of the velocity *u* and the Lorentz force F_L are shown in Fig. 9 and Fig. 10. The velocity vectors along the channel are given in Figs. 9 (a, b, c). As expected, the velocity vectors change in the flow direction over the entrance region, up to the region far from entry (fully developed region) that the velocity vectors have no further change in the flow direction. As well, it can be seen that as the Hartmann number increases the velocity vectors in the same cross section of the channel become flattened.

Figs. 10 (a, b, c) show the vectors of Lorentz force (F_L) along the channel. As discussed earlier, F_L is proportional to the velocity directly. Thus, the variation pattern of F_L in the flow direction is similar to the velocity. However, because F_L is the resistance force, affects in the opposite direction to the flow and velocity. Moreover, the velocity has maximum value in the centerline of the channel so the F_L is also maximum there. As well as, near the walls F_L decreases as the velocity reduces.

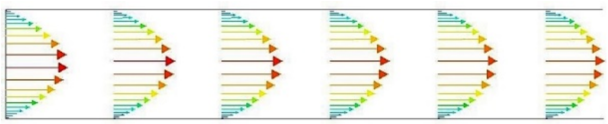

(a) Ha = 8

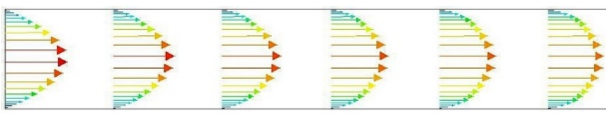

(b) Ha = 12

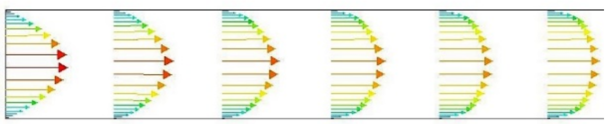

(c) Ha = 16

Fig. 9. Velocity vectors along the channel (Re = 1400)

The effect of the Reynolds and Hartmann numbers on the MHD fully developed centerline velocity and the MHD entrance length are shown in Fig. 11 and Fig. 12. It can be found that with increasing the Reynolds number both the fully developed centerline velocity and the MHD entrance length increase (Fig. 11). The Reynolds number is the ratio of the inertia to viscous forces. The augmentation of Re means the increase in inertia. Thus, the centerline velocity increases and the boundary layer growth is declined and therefore the flow becomes fully developed later.

As can be observed in Fig. 12, when the Hartmann number increases, the MHD fully developed centerline velocity and the MHD entrance length reduce. Increasing of Ha means an increase of Lorentz force, faster boundary layer growth, sooner fully developed condition and hence reduce of entrance length.

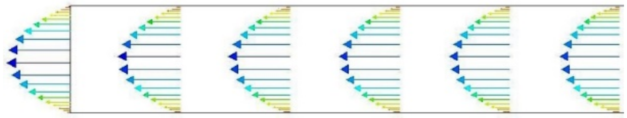

(a) Ha = 8

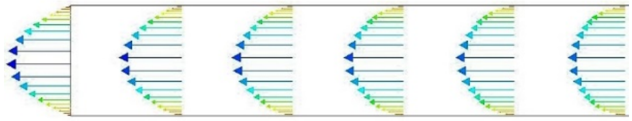

(b) Ha = 12

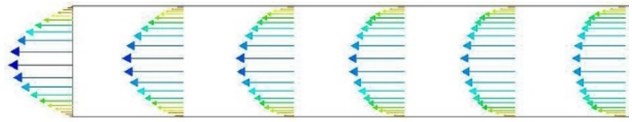

(c) Ha = 16

Fig. 10. The Lorentz force vectors along the channel (Re = 1400)

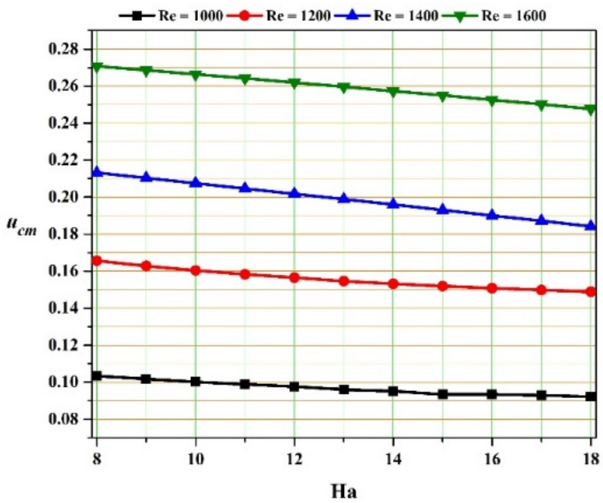

Fig. 11. Effect of Reynolds and Hartmann number on u_{cm}

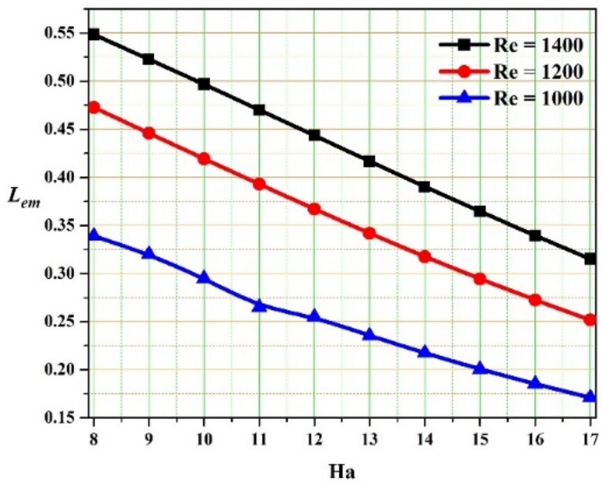

Fig. 12. Effect of Re and Ha on MHD entrance length

6. Conclusion

In this work, a solution based on the numerical finite volume method (FVM) and artificial neural networks scheme (ANNs) was successfully applied to investigate the two-dimensional magnetohydrodynamics channel developing flows. Correlations for prediction of the MHD channel flows entrance length were proposed. The values of the entrance length obtained from proposed correlations were compared with the literature validated data and a very good agreement was observed between them. The results were presented graphically and the effect of the governing parameters on the entrance length and the velocity profiles were discussed. It was concluded that with increasing of the Reynolds number, the entrance length increases. In contrast, the entrance length reduces when the Hartmann number increases. Also, it was found that with the increase of the Hartmann number, the velocity profile gets flattened and consequently, the entrance length becomes shorter.

Conflict of Interest

The authors declared no potential conflicts of interest with respect to the research, authorship and publication of this article.

Funding

The authors received no financial support for the research, authorship and publication of this article.

Nomenclature

B	Total magnetic field (T)	P	Gauge pressure (Pa)
B_0	External magnetic field (T)	Re	Reynolds number
b	Induced magnetic field (T)	u	x-component of the velocity (m/s)
E	Electric field (N/C)	u_c	Potential core centerline velocity (m/s)
F_L	Lorentz force (N)	u_{cm}	MHD fully developed centerline velocity (m/s)
Ha	Hartmann number	v	y-component of velocity (m/s)
J	Density of electric current (A/m^2)	x	Coordinate in the direction of flow (m)
L	Length of channel (m)	y	Coordinate in the direction normal to flow(m)
ℓ	Characteristic length (m)	ρ	Density (kg/m^3)
L_e	Entrance length (m)	σ	Electrical conductivity $(\Omega.m)^{-1}$
L_{em}	MHD entrance length (m)	μ	Dynamic viscosity (Pa.s)

References

[1] M. Javanmard, M.H. Taheri, S.M. Ebrahimi, Heat transfer of third-grade fluid flow in a pipe under an externally applied magnetic field with convection on wall, *Applied Rheology*, 28, 2018, 56023.
[2] M. Javanmard, M.H. Taheri, M. Abbasi, S.M. Ebrahimi, Heat transfer analysis of hydromagnetic water–graphene oxide nanofluid flow in the channel with asymmetric forced convection on walls, *Chemical Engineering Research and Design*, 136, 2018, 816-824.
[3] K. Hosseinzadeh, M. Alizadeh, D. Ganji, Hydrothermal analysis on MHD squeezing nanofluid flow in parallel plates by analytical method, *International Journal of Mechanical and Materials Engineering*, 13, 2018, 4.
[4] K. Hosseinzadeh, F. Afsharpanah, S. Zamani, M. Gholinia, D. Ganji, A numerical investigation on ethylene glycol-titanium dioxide nanofluid convective flow over a stretching sheet in presence of heat generation/absorption, *Case Studies in Thermal Engineering*, 12, 2018, 228-236.
[5] S.S. Ardahaie, A.J. Amiri, A. Amouei, K. Hosseinzadeh, D. Ganji, Investigating the effect of adding nanoparticles to the blood flow in presence of magnetic field in a porous blood arterial, *Informatics in Medicine Unlocked*, 10, 2018, 71-81.
[6] K. Hosseinzadeh, A.J. Amiri, S.S. Ardahaie, D. Ganji, Effect of variable lorentz forces on nanofluid flow in movable parallel plates utilizing analytical method, *Case Studies in Thermal Engineering*, 10, 2017, 595-610.
[7] A.S. Dogonchi, M. Alizadeh, D.D. Ganji, Investigation of MHD Go-water nanofluid flow and heat transfer in a porous channel in the presence of thermal radiation effect, *Advanced Powder Technology*, 28, 2017, 1815-1825.
[8] M. Rahimi-Gorji, O. Pourmehran, M. Gorji-Bandpy, D. Ganji, Unsteady squeezing nanofluid simulation and investigation of its effect on important heat transfer parameters in presence of magnetic field, *Journal of the Taiwan Institute of Chemical Engineers*, 67, 2016, 467-475.
[9] O. Pourmehran, M. Rahimi-Gorji, D. Ganji, Heat transfer and flow analysis of nanofluid flow induced by a stretching sheet in the presence of an external magnetic field, *Journal of the Taiwan Institute of Chemical Engineers*, 65, 2016, 162-171.
[10] P.G. Moakher, M. Abbasi, M. Khaki, Fully developed flow of fourth grade fluid through the channel with slip condition in the presence of a magnetic field, *Journal of Applied Fluid Mechanics*, 9, 2016, 2239-2245.
[11] O. Pourmehran, M. Rahimi-Gorji, M. Gorji-Bandpy, T. Gorji, Simulation of magnetic drug targeting through tracheobronchial airways in the presence of an external non-uniform magnetic field using Lagrangian magnetic particle tracking, *Journal of Magnetism and Magnetic Materials*, 393, 2015, 380-393.
[12] M.H. Taheri, M. Abbasi, M. Khaki Jamei, An integral method for the boundary layer of MHD non-Newtonian power-law fluid in the entrance region of channels, *Journal of the Brazilian Society of Mechanical Sciences and Engineering*, 39, 2017, 4177-4189.
[13] K.A. Helmy, H.F. Idriss, S.A. Kassem, An Integral Method For The Solution of The Boundary Layer Equation For Power-Law MHD Fluid, *Indian Journal of Pure and Applied Mathematics*, 32, 2001, 859-870.
[14] J.A. Lima, L.M. Pereira, E.N. Macêdo, C.L. Chaves, J.N.N. Quaresma, Hybrid solution for the laminar flow of power-law fluids inside rectangular ducts, *Computational Mechanics*, 26, 2000, 490-496.
[15] R.C. Gupta, Laminar two-dimensional entrance region flow of power-law fluids II, *Acta Mechanica*, 84, 1990, 209-215.
[16] R.E. Schwirian, A New Momentum Integral Method for MHD Channel Entrance Flows, *AIAA Journal*, 8, 1970, 565-567.
[17] A. Maciulatis, A.L.L. JR., A Theoretical Investigation of MHD Channel Entrance Flows, *AIAA Journal*, 2, 1964, 2100-2103.
[18] J.A. Lima, M.G.O. Rego, On the integral transform solution of low-magnetic MHD flow and heat transfer in the entrance region of a channel, *International Journal of Non-Linear Mechanics*, 50, 2013, 25-39.
[19] C.L. Hwang, K.C. Li, L.T. Fan, Magnetohydrodynamic Channel Entrance Flow with Parabolic Velocity at the Entry, *The Physics of Fluids*, 9, 1966, 1134-1140.
[20] F. Flores, A. Recuero, Magnetohydrodynamic entrance flow in a channel, *Applied Scientific Research*, 25, 1972, 403-

412.
[21] P.J. Bhuyan, K.S. Goswami, Effect of Magnetic Field on MHD Pressure Drop Inside a Rectangular Conducting Duct, *IEEE Transactions on Plasma Science*, 36, 2008, 1955-1959.
[22] M. Sahu, P. Singh, S.S. Mahapatra, K.K. Khatua, Prediction of entrance length for low Reynolds number flow in pipe using neuro-fuzzy inference system, *Expert Systems with Applications*, 39, 2012, 4545-4557.
[23] Y. Li, O. Zikanov, Laminar pipe flow at the entrance into transverse magnetic field, *Fusion Engineering and Design*, 88, 2013, 195-201.
[24] A. Patel, R. Bhattacharyay, P.K. Swain, P. Satyamurthy, S. Sahu, E. Rajendrakumar, S. Ivanov, A. Shishko, E. Platacis, A. Ziks, Liquid metal MHD studies with non-magnetic and ferro-magnetic structural material, *Fusion Engineering and Design*, 89, 2014, 1356-1361.
[25] C.N. Kim, Magnetohydrodynamic flows entering the region of a flow channel insert in a duct, *Fusion Engineering and Design*, 89, 2014, 56-68.
[26] P. Satyamurthy, P.K. Swain, V. Tiwari, I.R. Kirillov, D.M. Obukhov, D.A. Pertsev, Experiments and numerical MHD analysis of LLCB TBM Test-section with NaK at 1 T magnetic field, *Fusion Engineering and Design*, 91, 2015, 44-51.
[27] D. Chatterjee, S.K. Gupta, MHD flow and heat transfer behind a square cylinder in a duct under strong axial magnetic field, *International Journal of Heat and Mass Transfer*, 88, 2015, 1-13.
[28] D. Jasikova, M. Kotek, V. Kopecky, An effect of entrance length on development of velocity profile in channel of millimeter dimensions, *AIP Conference Proceedings*, 1745, 2016, 020018.
[29] Z. Kountouriotis, M. Philippou, G.C. Georgiou, Development lengths in Newtonian Poiseuille flows with wall slip, *Applied Mathematics and Computation*, 291, 2016, 98-114.
[30] K. Jambunathan, S.L. Hartle, S. Ashforth-Frost, V.N. Fontama, Evaluating convective heat transfer coefficients using neural networks, *International Journal of Heat and Mass Transfer*, 39, 1996, 2329-2332.
[31] N. Sözbir, İ. Ekmekçi, Experimental study and artificial neural network modeling of unsteady laminar forced convection in a rectangular duct, *Heat and Mass Transfer*, 43, 2007, 749-758.
[32] G. Díaz, M. Sen, K.T. Yang, R.L. McClain, Simulation of Heat Exchanger Performance by Artificial Neural Networks, *HVAC&R Research*, 5, 1999, 195-208.
[33] M. Carrillo, J.A. Gónzalez, U. Que, Estimation of the Reynolds number in a Poiseuille flow using artificial neural networks, *Journal of Physics: Conference Series*, 792, 2017, 012071.
[34] P.A. Davidson, *An Introduction to Magnetohydrodynamics*, Cambridge University Press, Cambridge, 2001.
[35] S. M. Ebrahimi, M. Javanmard, M. H. Taheri, M. Barimani, Heat transfer of fourth-grade fluid flow in the plane duct under an externally applied magnetic field with convection on walls, *International Journal of Mechanical Sciences*, 128–129, 2017, 564-571.
[36] H. Schlichting, *Boundary-Layer Theory*, 8th rev. and enl. ed., Springer, Berlin, 2000.
[37] I.E. Lyublinski, A.V. Vetkov, V.A. Evtikhin, Application of lithium in systems of fusion reactors. 1. *Physical and chemical properties of lithium, Plasma Devices and Operations*, 17, 2009, 42-72.
[38] Z. Duan, Y.S. Muzychka, Slip Flow in the Hydrodynamic Entrance Region of Circular and Noncircular Microchannels, *Journal of Fluids Engineering*, 132, 2009, 011201-011201-011213.
[39] R.E. Nygren, T.D. Rognlien, M.E. Rensink, S.S. Smolentsev, M.Z. Youssef, M.E. Sawan, B.J. Merrill, C. Eberle, P.J. Fogarty, B.E. Nelson, D.K. Sze, R. Majeski, A fusion reactor design with a liquid first wall and divertor, *Fusion Engineering and Design*, 72, 2004, 181-221.

ORCID iD

Mohammad Hasan Taheri https://orcid.org/0000-0003-1811-4404
Nematollah Askari https://orcid.org/0000-0003-3338-0954
Mohammad Hadi Mahdavi https://orcid.org/0000-0001-7797-5082